JOURNAL OF MATERIALS SCIENCE 26 (1991) 2100–2106

Effect of fibre surface treatment on yielding and fracture behaviour of glass fibre–polypropylene composite

V. DI LIELLO, E. MARTUSCELLI, G. RAGOSTA, A. ZIHLIF*
Istituto di Ricerche su Tecnologia dei Polimeri e Reologia del C.N.R., Via Toiano 6, 80072 Arco Felice (Napoli) Italy

Two parallel studies of the mechanical properties of composites based on modified polypropylene is presented. The fillers used were either uncoated-glassy fibres or glassy fibres coated with aluminium. The tensile properties and fracture behaviour are investigated as a function of filler content over a range of temperatures and strain rates. The measured elastic modulus, tensile strength, and fracture parameters, G_c and K_c, showed dependencies on filler content. The observed enhancement is found to be remarkable in the case of composites containing uncoated surface treated glass fibres. The tensile yield stress of all the composites prepared showed strain rate and temperature dependence. Stress activation volume and activation energy of single-activated yielding processes are determined. The observed fracture morphology could explain the reinforcement behaviour of the measured mechanical properties.

1. Introduction

Advanced composite materials are widely used in modern electronic and communication technologies as well as in aerospace and military applications [1–3]. In general, these materials contain high performance fibres like carbon and aramid fibres embedded in a polymeric matrix. Other common composites include steel fibres or carbon black to promote high electrical performance and good electromagnetic interference (EMI) for shielding properties. Thermoplastic matrices such as polypropylene also find application in the field of high performance composite materials [4–7].

This paper is the first part of a series concerned with the electrical and mechanical behaviour of glass fibre reinforced polypropylene composites which were formulated with the aim of obtaining good mechanical, electrical and EMI properties [8–13]. In particular the effect of aluminium fibre coating is investigated in a wide range of temperatures and strain rates to better understand the role played by the interfacial adhesion in the mechanical properties of these materials. Finally the correlations among the fracture behaviour and the morphology of these systems are discussed.

2. Experimental details

2.1. Materials and composite preparation

The materials used in the present study are: (1) isotactic polypropylene (PP) (Mn = 58 000, Mw = 275 000, Mw/Mn = 4.74); melt index = 10 g min^{-1}. Acrylic acid modified isotactic polypropylene (PP*) obtained [6] by melt-mixing the PP with 2% (by weight) of acrylic acid at $T = 190\,^{\circ}C$; (2) aluminium coated-glass fibres; (3) uncoated-glass fibres. These fibres have average diameters of 13 μm and were used as composite filler. They were provided by MARBO S.p.A. -Milano (Italy) on mat form; the fibre strands were chopped into single filaments of an average length of 1 mm. The two fibre categories, coated and uncoated, are treated with a silane coupling agent in order to promote the adhesion between the matrix and the fibres. The matrix used was a mixture made of 90% (by weight) of PP and 10% (by weight) of PP*. The short chopped fibres were mixed with this modified PP matrix using a Brabender-like apparatus (Rheocord EC of Haake Inc.) operating at a moulding temperature of 200 °C and a residence time of 10 min. This procedure was then followed by hot compression moulding at 200 °C. The composite plates obtained have thicknesses of 4 mm and 1.3 mm. The glass fibre content in these composites are: 5, 10, 20 and 30 wt %.

2.2. Tensile tests

To study the tensile deformation behaviour of these composite materials, dumb-bell specimens were cut from the 1.3 mm sheets. Tensile tests were performed by an Instron testing machine equipped with an environmental chamber to work at different temperatures and over a range of strain rates. Temperature readings were taken by placing a thermometer near the test specimen.

*On sabbatical leave from the Physics Department of the University of Jordan, Amman, Jordan

0022–2461/91 $03.00 + .12

2.3. Impact fracture tests

Fracture tests were carried out on a Charpy Instrumented Pendulum (Ceast Autographic Pendulum MK2), at an Impact speed of 1 $m\,s^{-1}$. Samples with a notch depth to width ratio of 0.3 and test span of 48 mm were fractured at room temperature. The relative curves of energy and load versus time or displacement were recorded.

2.4. Microscopy and X-ray diffraction

Adhesion and morphological investigations were carried out using a Philips 501 scanning electron microscopy (SEM) on fracture surfaces obtained by tensile and impact tests. The samples for SEM observations were metallized by means of Polaron sputtering apparatus with Au–Pd alloy. Optical examinations were carried out using a Wild M420 Stereomicroscope. The X-ray diffraction (XRD) patterns obtained for the PP matrix were concentric rings, indicating isotropy. Thus no matrix orientation was observed during the compression moulding.

3. Results and discussion

3.1. Tensile Results

The stress–strain measurements obtained at a strain-rate $\dot{\varepsilon} = 7.4 \times 10^{-3}\,s^{-1}$ for the various prepared composites showed a ductile plastic deformation behaviour. It was noticed that by increasing the fibre concentration, the degree of brittleness increased. This is accounted for by the presence of brittle glass fibres embedded in a ductile modified polypropylene matrix. The dependence of the Young's modulus (E), on the fibre content for both aluminium-coated and uncoated-glass fibre composites, is shown in Fig. 1. It can be seen that the stiffness of the material increases slowly with the fibre content for the coated-glass fibre composites, while showing a more pronounced effect in the case of the uncoated-glass fibre composites.

Fig. 2 shows the variations of the yield stress (σ_y) as a function of the glass fibre content. This parameter decreases linearly for coated-fibre composites whereas

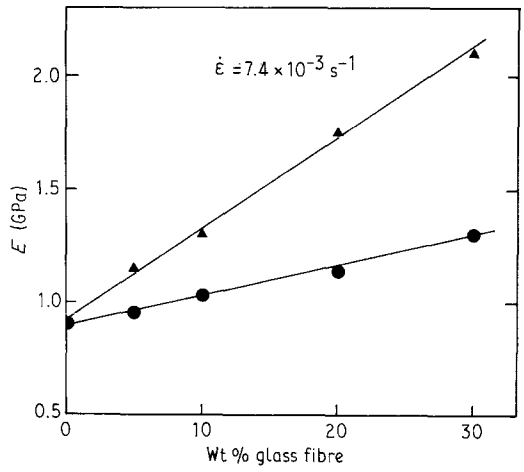

Figure 1 Young's modulus of glass fibre reinforced polypropylene as a function of fibre content: (▲) uncoated-fibres; (●) coated-fibres, $\dot{\varepsilon} = 7.4 \times 10^{-3}\,s^{-1}$.

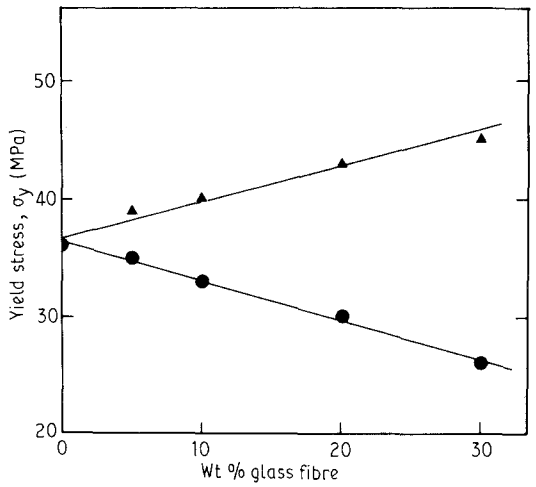

Figure 2 Tensile yield stress of polypropylene–glass fibre composite as a function of fibre content: (▲) uncoated-fibres; (●) coated-fibres, $T = 20\,°C$.

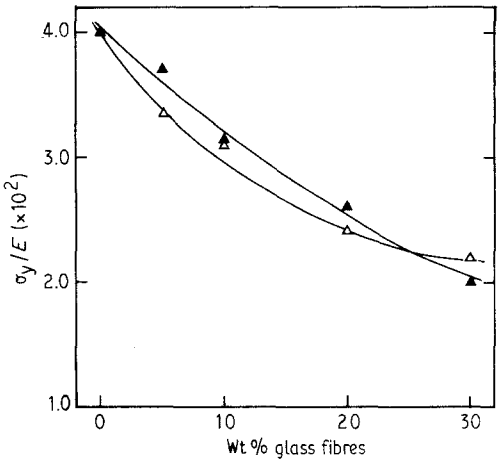

Figure 3 Yield stress/Young's modulus ratio as a function of glass fibre content: (△) uncoated-fibres; (▲) coated-fibres.

an opposite trend is observed in the case of the uncoated-glass fibre composites. The gradual decrease of σ_y found for the coated-glass fibres is most likely due to weak interfacial bonding with the PP matrix. In fact, although the coated-fibres were surface treated with the silane coupling agent, the chemical interaction between the fibre surface and the matrix was hindered by the presence of aluminium-coating particles. The ratio of the yield stress to Young's modulus for the various investigated materials is plotted in Fig. 3 as a function of the glass fibre content. The σ_y/E ratio decreases by increasing the glass fibre content; a similar result has been obtained by us in the case of polypropylene/carbon fibre composites [11]. This parameter behaves similarly for both the coated and the uncoated systems even though the yield stress dependence on the fibre content is different. The average value of the σ_y/E ratio at a strain rate of $\dot{\varepsilon} = 7.4 \times 10^{-3}$ and 20 °C is about 0.03 which is close to the values quoted in the literature for typical polymers [14, 15]. The observed variations in σ_y/E within a small range [0.04–0.02] imply that the overall deformation behaviour of the composites is still physically dominated by the elastic–plastic properties of the PP matrix.

Stress–strain curves were also obtained over a range of temperatures and strain rates for various prepared PP composites. Figs 4 and 5 show the dependence of the tensile yield stress on temperature for coated and uncoated composites, respectively. In both cases the yield stress decreases linearly with increasing temperature. The tensile yield stress, for 0, 5, 10, 20, and 30 wt % composite specimens, measured at room temperature, is plotted as a function of the logarithm of the strain rate in Figs 6 and 7. The data show a linear relationship between σ_y and the strain rate for polypropylene and for all the investigated composites. The observation that the straight lines are not parallel indicates the occurrence of multiple rate activated processes. This, can be explained by the Eyring model, which considers the yielding as a rate activated phenomenon resulting from the segmental motion of the polymer molecules [14–17].

Such a model describes the dependence of the yield stress on strain rate ($\dot{\varepsilon}$) and absolute temperature T in terms of the following equation

$$\dot{\varepsilon} = \varepsilon_0 \exp - (E_a - \sigma_y V^*)/KT \quad (1)$$

where $\dot{\varepsilon}_0$ is constant, E_a is the activation energy for rate activated process, σ_y is the yield stress, V^* is the stress activation volume, K is the Boltzmann constant, and T is the absolute temperature. This equation implies that the stress at yield and the logarithm of strain rate have a linear relationship with a slope given by

$$[\partial\sigma_y/\partial \ln\dot{\varepsilon}]_T = KT/V^* \quad (2)$$

The values of the activation energy and the activation volume are calculated from the observed linear dependence of Figs 6 and 7 for the PP polymer and for all the investigated composites. Figs 8 and 9 show the variations of both the activation volume V^* and the activation energy E_a as a function of the weight fraction of aluminium-coated and uncoated-glass fibres. It can be seen that V^* increases with the fibre content in the former case, while it decreases in the latter. This trend is due to the fact that, as discussed above, the yield stress decreases for the coated-composites and increases for the uncoated-ones.

The activation energy values for the uncoated-fibre composites remain almost constant ($\sim$ 38 kcal mol^{-1}) at relatively low fibre contents, and decrease slightly to about 33 kcal mol^{-1} when the amount of glass fibres reach a value of 30 wt %

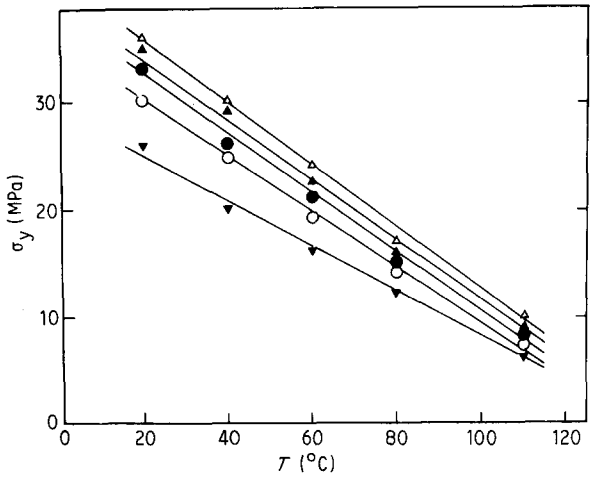

Figure 4 Variations of the yield stress with temperature for coated-fibre composites: (△) modified polypropylene, (▲) 5 wt %, (●) 10 wt %, (○) 20 wt % and (▼) 30 wt %.

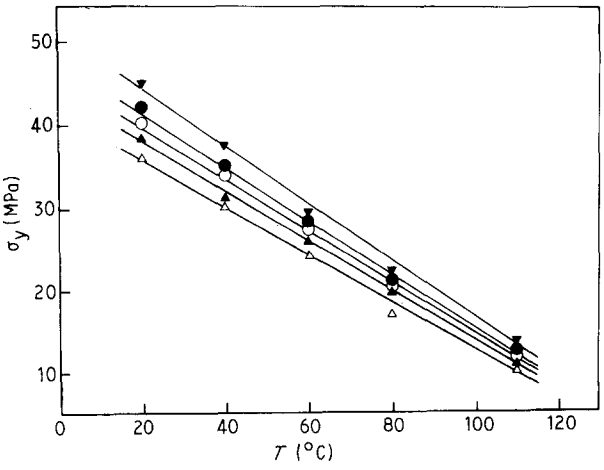

Figure 5 Variations of the yield stress with temperature for uncoated-fibre composites. (Symbols as in Fig. 4, $\dot{\varepsilon} = 7.4 \times 10^{-3} s^{-1}$)

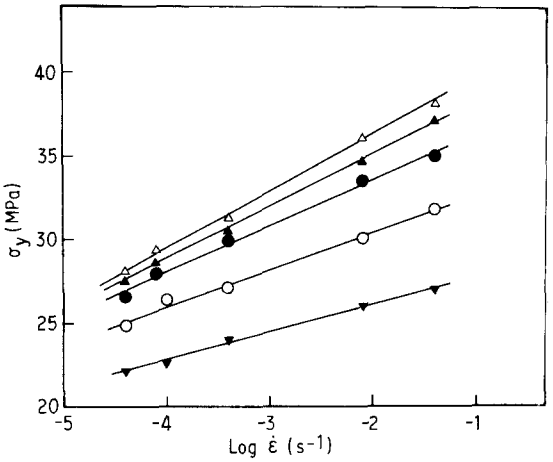

Figure 6 Dependence of the yield stress on strain rate at room temperature for coated-fibre composites: (△) 0 wt %, (▲) 5 wt %, (●) 10 wt %, (○) 20 wt %, and (▼) 30 wt %, carbon fibre content, $T = 20\,°C$.

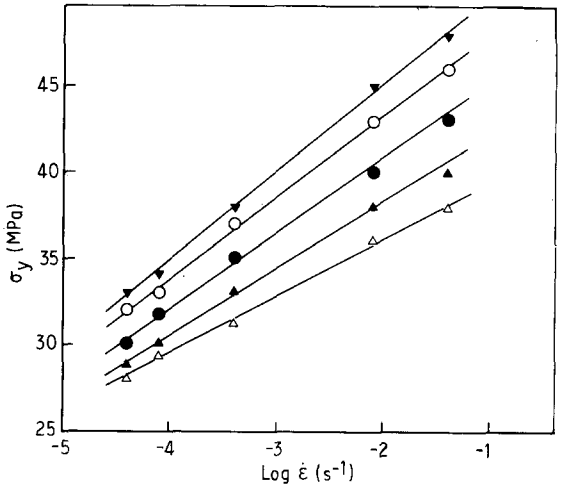

Figure 7 Dependence of the yield stress on strain rate at room temperature for uncoated-fibre composites. (Symbols as in Fig. 6).

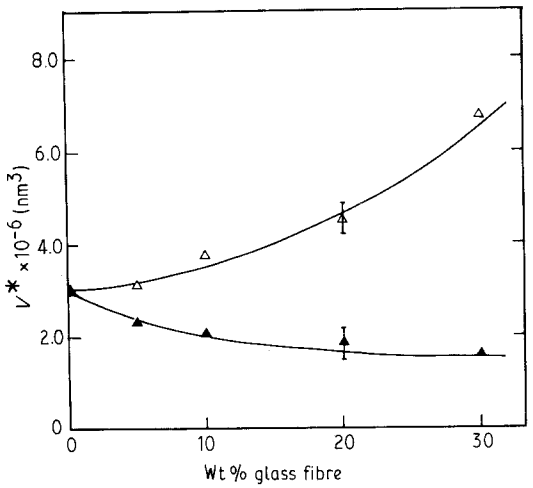

Figure 8 Variations of the stress activation volume as a function of the glass fibre content: (▲) uncoated-fibres; (△) coated-fibres.

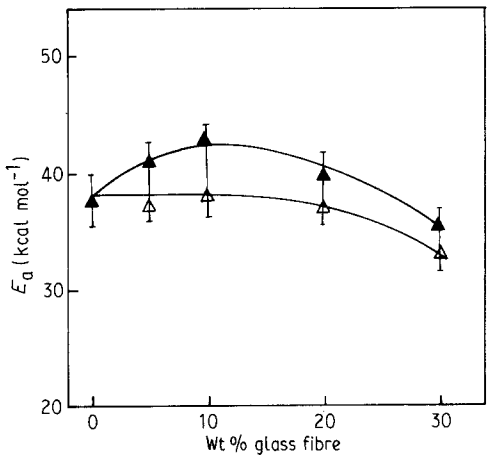

Figure 9 Variation of the activation energy as a function of the glass fibre content: (△) uncoated-fibres; (▲) coated-fibres.

(see Fig. 9). The behaviour of E_a is slightly different for the coated-fibre composites: a maximum of ~ 42 kcal mol^{-1} is observed in this case at a fibre content of 10 wt %. It has to be stressed that several investigators have found either a very slight decrease or an approximate independence of E_a on the filler content in a wide variety of composite materials [11, 18, 19]. In our case the effect is only slightly above the experimental uncertainty with which the E_a values are determined. Certainly it is not straightforward to predict the behaviour of E_a as a function of the filler content since several effects must be taken into account. For instance the yielding phenomenon is strongly dependent on the type of filler as well as on the molecular structure of the matrix [20, 21]; all this will effect, in a peculiar fashion, the E_a behaviour as a function of filler content in these materials. Moreover a more accurate determination of the E_a values is required, based on improved experimental techniques as well as on a statistical treatment of the rough data.

3.2. Impact fracture results

3.2.1. Fracture toughness parameters

The critical stress intensity factor, K_c, is calculated using the fracture mechanics approach [22–26] from the equation

$$K_c = \sigma Y a^{1/2} \quad (3)$$

where σ is the nominal stress at the onset of crack propagation, a is the initial crack length and Y is a calibration factor depending on the specimen geometry.

For the determination of the critical strain energy release rate, G_c, the following equation is used

$$G_c = U/bw\phi \quad (4)$$

where U is the fracture energy corrected from the kinetic energy contribution, b and w are thickness and the width of the specimen and ϕ is a calibration factor which depends on the length of crack and size of the sample. The values of ϕ were taken from Plati and Williams [25].

3.2.2. Fracture toughness results

The critical stress intensity factor (K_c) measured as a function of coated and uncoated-glass fibre content at room temperature is shown in Fig. 10. The K_c increases linearly with the fibre content for both types of composites. However the effect is more pronounced for the uncoated-glass fibre samples.

This larger enhancement of K_c, is essentially due to the fact that in the case of uncoated-glass fibre samples, a higher interfacial bonding exists between the fibre and the matrix, as will be evinced by the fractographic analysis reported in the next section. A similar behaviour is observed for the critical strain energy release rate (G_c) (see Fig. 11).

4. Morphology–Property considerations

Optical observations of the moulded-specimens showed smooth surfaces without pores or voids and an even distribution of the glass fibres within the matrix. The tensile deformation of the investigated samples was characterized by a yielding phenomenon starting with the appearance of wavy crazes and whiteness, followed by shear banding, and finally by failure with relatively straight edge transverse cracks.

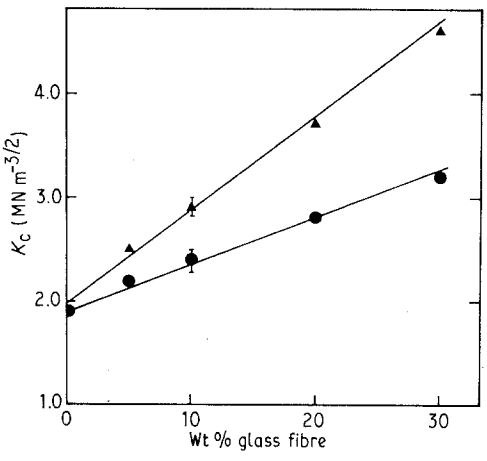

Figure 10 Critical stress intensity factor (K_c) as a function of glass fibre content: (▲) uncoated-fibres; (●) coated-fibres.

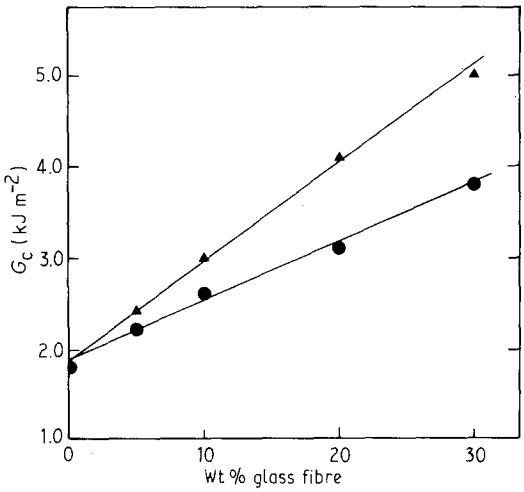

Figure 11 Critical strain energy release rate (G_c) as a function of fibre content: (▲) uncoated-fibres; (●) coated-fibres.

The observed increase in stiffness, yield stress and fracture toughness with coated and uncoated-glass fibre content, discussed previously, may be related to some morphological features observed by SEM analysis.

Fig. 12 shows scanning electron micrographs of fractured surfaces of different fibre coated composites obtained during the fracture tests. It can be seen that a fraction of the glass fibres are partially implanted in the PP matrix while others are not covered by the matrix and are pulled out during the fracture process especially at higher fibre concentrations (20 and 30 wt %). This indicates that coated-fibres are not bound very well to the matrix because the aluminium-coating particles prevent any contact or interaction between the silane coupling agent and the surface of the glass fibres.

The situation seems to be different in the case of the uncoated-glass fibre composites. Fig. 13 shows SEM micrographs of fractured surfaces where the fibres are well bounded to the PP matrix without voids around them. Three morphological features are also evident in Fig. 13: (1) a remarkable plastic deformation of the PP matrix; (2) well implanted and embedded fibres without pulling-out, and (3) the PP matrix partially covering the fibres after the fracture. This type of morphology certainly indicates an excellent interfacial bonding between the fibres and the matrix.

The observed morphology can explain the fracture toughness enhancement found in these systems. In particular the observed effect can be attributed to composite lamination where the applied stress is suddenly accommodated and the impact energy is dispersed through the composite bulk. Thus, during fracture, the amount of energy required to form voids and cracks at the fibre–matrix interface increases with increasing glass–fibre network supporting the applied

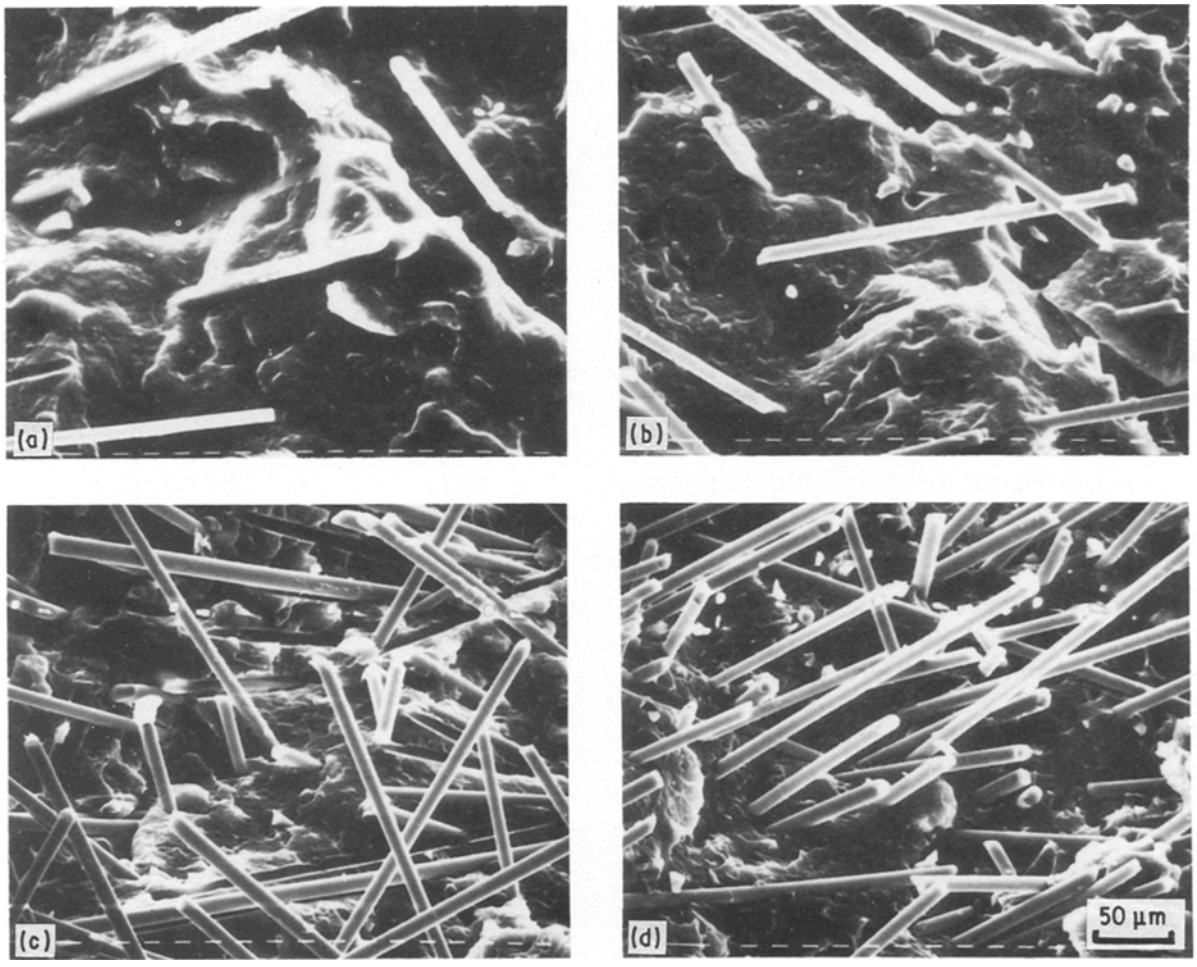

Figure 12 Scanning electron micrographs of coated composite specimens fractured under impact tests: (a) 5 wt % glass fibres; (b) 10 wt % glass fibres; (c) 20 wt % glass fibres; (d) 30 wt % glass fibres.

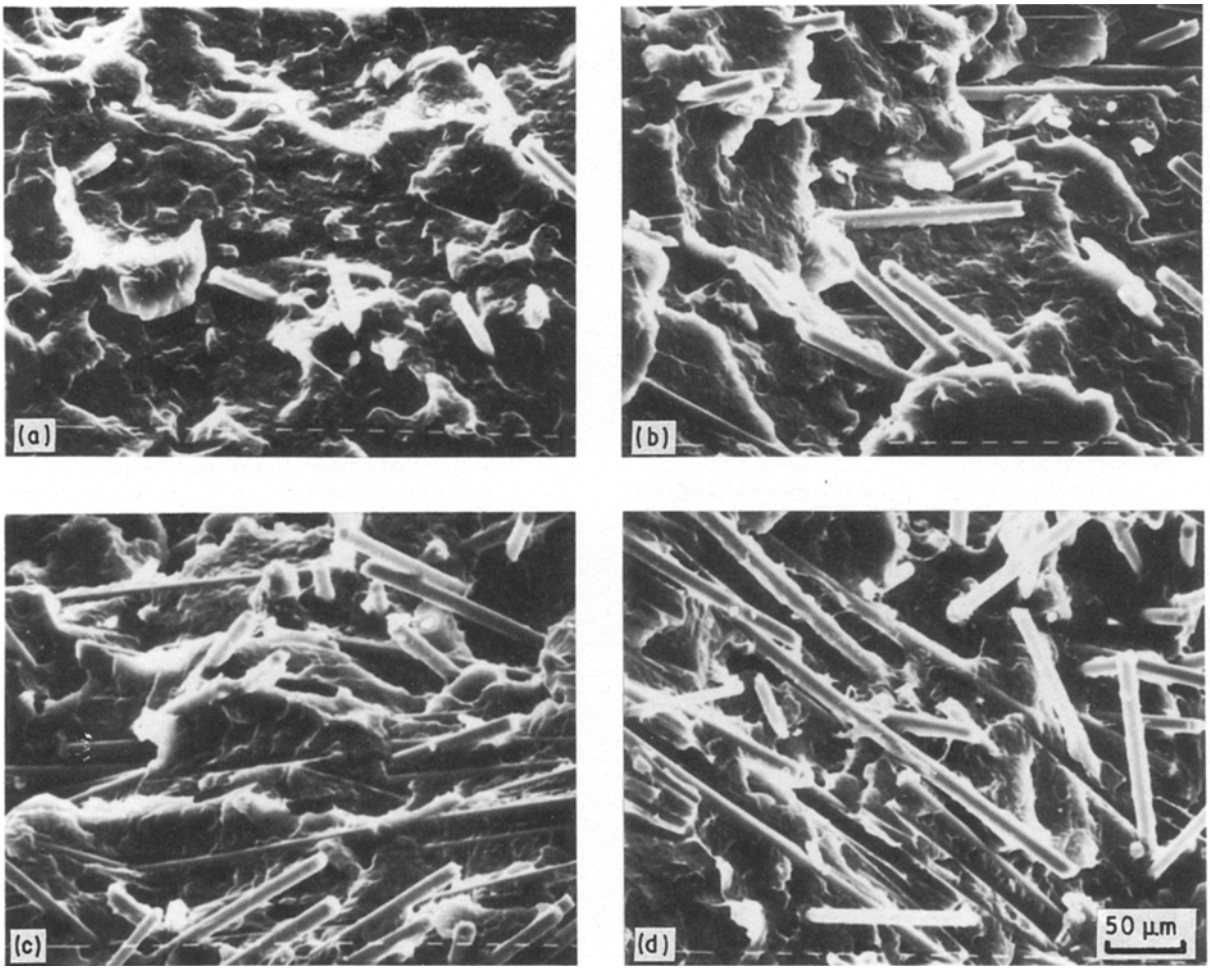

Figure 13 Scanning electron micrographs of uncoated composites specimens fractured under impact tests: (a) 5 wt % glass fibres; (b) 10 wt % glass fibres; (c) 20 wt % glass fibres; (d) 30 wt % glass fibres.

loads, particularly in the crack-tip zone characterized by a large amount of plastic deformation [26]. This condition can be achieved either by increasing the amount of glass fibres in the polymeric matrix, with a relatively low enhancement of the fracture parameters or by increasing the fibre concentration with a certain surface-fibre treatment which yields a more substantial increase in these parameters as in the case of the uncoated-fibre composites (Figs 10 and 11).

5. Conclusion

Polypropylene based composites reinforced with aluminium-coated/uncoated-glass fibres were prepared to study the changes in tensile properties and fracture toughness with filler content over a range of temperatures and strain rates. Mechanical properties are correlated with the observed morphology of the fractured samples in an attempt to shed light on the yielding phenomenon and fracture. The following conclusions can be drawn from the results obtained:

1. The elastic modulus of all composites increases by enhancing the fibre content; it increases more rapidly in the case of the uncoated-fibre composites.

2. The tensile yield stress shows a temperature, strain rate and fibre content dependence. The yield stress decreases with the fibre content for the coated-fibre composites while showing an opposite trend for the uncoated-fibre systems.

3. The calculated stress activation volume increases with the coated-fibre content and decreases in the case of the uncoated-fibre composites. The activation energy shows slight changes for all the investigated composites.

4. The fracture toughness parameters (K_c) and (G_c) increase with the glass fibre content and shows a higher increasing rate in the case of uncoated-fibre composites.

5. The fracture process is associated with large plastic deformations due to good interfacial fibre/matrix bonding in the case of uncoated-composites, while for the coated-composites a small amount of plastic deformation is observed.

6. The observed morphology explains the reinforcement effects on the mechanical and fracture properties.

Acknowledgements

One of the authors (A.Z.) is very grateful to both the International Centre for Theoretical Physics at Triest (Italy), and the University of Jordan (Amman) for financial support. We thank Dr. A. Abate for providing the glass fibre samples. This work has been

partially supported by C.N.R. "Progetto Finalizzato Chimica Fine II".

References

1. G. LUBIN, in "Handbook of Composites" (Van Nostrand Corporation, London, 1982).
2. M. A. MEYERS and O. T. INAL, in "Frontiers in Materials Technologies" (Elsevier, Amsterdam, 1985) Ch. 12.
3. R. M. GILL, in "Carbon Fibers in Composites Materials" (The Plastic Institute, London, 1972).
4. M. TAKAYANAGI, *Polymer* **19** (1987) 21.
5. C. L. LHYMAN and J. M. SCHULTZ, *Composites* **8** (1987) 287.
6. M. AVELLA, E. MARTUSCELLI, C. SELLITTI and E. GARAGNANI, *J. Mater. Sci.* **22** (1987) 3185.
7. J. U. OTAIGBE and W. G. HARLAND, *J. Appl. Polym. Sci.* **36** (1988) 165.
8. Z. OSAWA and K. KOBYASHI, *J. Mater. Sci.* **22** (1987) 4381.
9. M. K. ABDELAZEER, M. S. ABMAD and A. M. ZIHLIF, *ibid.* **24** (1989) 1309.
10. F. J. BALTA CALLEJA, R. A. BAYER and T. A. EZOUERRA, *ibid.* **23** (1988) 1411.
11. V. DI LIELLO, E. MARTUSCELLI, G. RAGOSTA and A. ZIHLIF, *ibid.* **25** (1990) 706.
12. M. S. AHMAD, M. K. ABDELAZEEZ, A. ZIHLIF, E. MARTUSCELLI, G. RAGOSTA and E. SCAFORA, *ibid.* in press.
13. M. S. AHMAD, M. K. ABDELAZEEZ, A. M. ZIHLIF, E. MARTUSCELLI, G. RAGOSTA and E. SCAFORA, *Polymer Composites*, in press.
14. B. HARTMANN, G. F. LEE and R. F. COLE, *Polym. Eng. Sci.* **27** (1987) 823.
15. N. BROWN, in "Failure of Plastics", edited by W. Brostow and R. D. Cornelliussen, Ch. 6 (Hanser Publishers, Munich, 1986).
16. I. M. WARD, *J. Mater. Sci.* **6** (1971) 1397.
17. T. K. MATTIOLI and D. J. QUESNEL, *Polym. Eng. Sci.* **27** (1987) 848.
18. M. SUMITA, V. TSUKUMO, K. MIYASAKA and K. ISHIKAWA, *J. Mater. Sci.* **18** (1983) 1758.
19. S. S. BHAGAWAN and S. K. DE, *Polym. Plast. Technol. Eng.* **27** (1983) 37.
20. S. N. MAITI and P. K. MAHAPATRO, *J. Appl. Polym. Sci.* **37** (1989) 1889.
21. V. KHUNOVA, V. SMATKO, I. HUDEC and A. BENISKA, *Prog. Colloid Polym. Sci.* **78** (1988) 188.
22. J. G. WILLIAMS, in "Fracture Mechanics of Polymers" (Ellis Horwood Limited, New York, 1984) pp. 238–292.
23. A. J. KINLOCH and R. I. YOUNG, in "Fracture Behaviour of Polymers" (Applied Science Publishers, London, 1983) pp. 74–106.
24. R. GRECO and G. RAGOSTA, *Plast. Rubb. Proc. Appl.* **7** (1987) 163.
25. E. PLATI and J. G. WILLIAMS, *Polym. Eng. Sci.* **15** (1975) 470.
26. R. GRECO and G. RAGOSTA, *J. Mater. Sci.* **23** (1988) 4171.

Received 23 November 1989
and accepted 24 April 1990